ResearchGate

See discussions, stats, and author profiles for this publication at: https://www.researchgate.net/publication/14162585

Apical and basolateral expression of Aquaporin-1 in transfected MDCK and LLC-PK cells and functional evaluation of their transcellular osmotic water permeabilities

ARTICLE in PFLÜGERS ARCHIV - EUROPEAN JOURNAL OF PHYSIOLOGY · MAY 1997

Impact Factor: 4.1 · DOI: 10.1007/s004240050345 · Source: PubMed

CITATIONS
45

READS
8

4 AUTHORS, INCLUDING:

Peter M T Deen
Radboud University Medical Centre (Radboudumc)

167 PUBLICATIONS **5,854** CITATIONS

SEE PROFILE

Available from: Peter M T Deen
Retrieved on: 25 January 2016

Pflügers Arch – Eur J Physiol (1997) 433:780–787 © Springer-Verlag 1997

ORIGINAL ARTICLE

Peter M. T. Deen · Søren Nielsen · René J. M. Bindels
Carel H. van Os

Apical and basolateral expression of Aquaporin-1 in transfected MDCK and LLC-PK cells and functional evaluation of their transcellular osmotic water permeabilities

Received: 9 October 1996 / Received after revision: 3 January 1997 / Accepted: 8 January 1997

Abstract Aquaporin-1 is present in the apical and basolateral membranes in proximal tubules and descending limbs of Henlé's loop. In order to be able to study the routing of Aquaporin-1 and the regulation of Aquaporin-1-mediated transcellular water flow, we stably transfected LLC-PK_1 and MDCK-HRS cell lines with an Aquaporin-1 expression construct. LLC-PK_1 clone 7 and MDCK clone K integrated two and one copies, respectively, which was reflected in the amount of *Aquaporin-1* mRNA expressed in both clones. The Aquaporin-1 protein levels, however, were similar. In both clones, immuno-electronmicroscopy showed extensive labelling of Aquaporin-1 on the basolateral plasma membrane, endosomal vesicles and the apical plasma membrane, including the microvilli. To measure transcellular water permeation, a simple method was applied using phenol-red as a cell-impermeant marker of concentration. In contrast to the native cell lines, both clones revealed a high transcellular osmotic water permeability, which could not be influenced by forskolin add/3-isobutyl-1-methylxanthine (IBMX) or the phorbol ester 12-*O*-tetradecanoyl 13-acetate (TPA). After glutaraldehyde fixation, it was inhibitable by $HgCl_2$. These results indicate that targeting of Aquaporin-1 to the apical and basolateral plasma membrane is independent of cell type and show for the first time that water flow through a cultured epithelium can be blocked by mercurial compounds.

Key words Water channel · Transfection · Kidney · Transcellular osmotic transport · Aquaporin-1 · Protein routing

P. M. T. Deen (✉) · R. J. M.Bindels · C. H.van Os
162, Department of Cell Physiology, University of Nijmegen, PO Box 9101, NL-6500 HB Nijmegen, The Netherlands

S. Nielsen
Department of Cell Biology, University of Aarhus, DK-8000 Aarhus C, Denmark

Introduction

Diffusional water permeability through the lipid bilayer is a characteristic of all cell membranes, but the high facilitated water permeability of renal cells has been attributed to several water channels expressed in specific segments of the nephron. The archetypal molecular water channel Aquaporin-1 (AQP1) is constitutively expressed at the basolateral and apical membranes of proximal tubules and descending limbs of Henlé's loop [34, 40] and is thought to account for 90% of the reabsorption of the glomerular filtrate [1]. In principal cells of the collecting duct and in inner medullary collecting duct (IMCD) cells, three additional water channels have been identified [15, 18, 20, 23]. AQP2 was shown to be predominantly present in subapical vesicles, which, upon activation of the V_2-receptor with vasopressin, fuse with the apical membrane of these cells [35]. AQP2 is implicated in an autosomal form of nephrogenic diabetes insipidus, a disease characterized by the inability of the kidney to concentrate urine in response to vasopressin [7, 28]. The basolateral membranes of principal and IMCD cells contain AQP3, a water channel that is also permeable to urea and glycerol, and which presumably provides an exit pathway for water and urea in antidiuresis [10, 20]. AQP4 is also present in basolateral membranes of collecting duct principal cells [43]. Although AQP1–4 are proposed to have similar membrane topologies, they are apparently targeted to different cellular destinations.

To be able to study targeting of aquaporins and regulation of transcellular water transport conferred by these proteins in epithelial cells, we have established stably transfected LLC-PK_1 and MDCK cells, which express AQP1 water channels, have used a simple technique to study transcellular water transport and have analysed the effects of mercurial compounds, protein kinase A (PKA) and protein kinase C (PKC) on the transcellular water transport mediated by AQP1.

Materials and methods

Expression construct

For high-level expression of AQP1, pSG5H*AQP1* (Fig. 1) was constructed as follows: as an insertion vector, pSG5H was obtained by ligating a 2.0-kbp *Sal*I *hygroB*^{r} cassette into the unique *Sal*I site of eukaryotic expression vector pSG5 [17]. The *hygroB*^{r} cassette consisted of a 1.8-kbp *Pvu*II/*Bgl*II fragment of vector pECV6 [2] containing the thymidine kinase (tk) promoter, the entire coding sequence of the *hygroB*^{r} gene, the tk polyadenylation signal and, at the 5'-end, a 180-bp *Eco*RI fragment spanning the polyoma mutant enhancer region, EPyF441 [14], derived from plasmid pMC1*Neo* [44]. Next, a 1044-bp *Sac*I–*Apa*I fragment, containing the entire coding region of rat AQP1 [6] was blunted and cloned into the blunted *Bam*HI site of pSG5H. With this cloning, the *Bam*HI sites flanking the AQP1 cDNA insert are restored. The cloning steps and the correct orientation of the inserted fragments were validated by restriction enzyme digestions. In vivo expression of *AQP1* mRNA from pSG5H*AQP1* is under control of the SV40 early promoter.

Cell culture and transfection

MDCK-HRS and LLC-PK$_1$ cells were grown in DME medium supplemented with 5% (v/v) fetal calf serum at 37°C in 5% CO_2. Transfection was carried out using the calcium-phosphate precipitation method [16]. Briefly, 24 h before transfection, cells were seeded at a density of $1 \cdot 10^6$ cells/90-mm dish. The medium of the cells was refreshed 2 h before transfection. 10 µg pSG5H*AQP1* was linearized by digestion with *Xba*I, purified by Sephacryl S-500 column chromatography, mixed with 10 µg sheared human carrier DNA, extracted with phenol-chloroform and chloroform, precipitated, washed twice with cell-culture-grade 70% ethanol and resuspended in 437 µl 0.1 × TE (10 mM Tris-HCl (pH=8.0); 1 mMEDTA). After addition of 63 µl of 2 M $CaCl_2$, 500 µl of 2 × HEPES-buffered saline (280 mM NaCl, 10 mM KCl, 1.5 mM Na_2HPO_4, 12 mM dextrose, 50 mM HEPES; pH=7.05) was slowly added under vigorous stirring, the DNA was allowed to precipitate for 20 min at 0°C and was subsequently added dropwise to the cells. The cells were incubated at 37°C in a humidified environment with 5% CO_2 for 6 h, washed with 10 ml Tris-buffered saline (TBS; 140 mM NaCl, 5 mM KCl, 0.6 mM Na_2HPO_4, 25 mM Tris; pH=7.5), shocked with 10 ml 20% (v/v) glycerol in TBS for 3 min at room temperature, washed with 10 ml TBS and fed with 8 ml medium. Then, 24 h after transfection and subsequently every 3–4 days, transfected LLC-PK$_1$ and MDCK cells were fed with medium containing 300 and 75 µg/ml hygromycin B (ICN Biochemicals), respectively. Then, 10–14 days after transfection, individual colonies were selected and expanded.

Southern blot analysis

Approximately 10 µg of isolated genomic DNAs was digested with *Bam*HI, fractionated on a 1% (w/v) agarose gel and transferred to Hybond (Amersham). To be able to estimate the copy number of pSG5H*AQP1* constructs integrated into the genome of the transfected cells, plasmid pSG5H*AQP1* was also digested with *Bam*HI. Equivalents corresponding to approximately 0.1, 1, 10 or 100 pg of the *AQP1* cDNA insert, each mixed with 10 µg *Bam*HI-digested LLC-PK$_1$ genomic DNA, were loaded onto the same gel. The above-mentioned *AQP1* cDNA fragment was labelled with [α-^{32}P]dCTP by random priming and used as a probe. Hybridization was done in hybridization buffer (250 mM Na_2HPO_4, 7% SDS, 1 mM EDTA, pH=7.2) at 65°C for 16 h. Subsequently, the filters were washed twice at 65°C in generous quantities of hybridization wash buffer (40 mM Na_2HPO_4, 0.1% SDS, 1 mM EDTA) and autoradiographed. The obtained signals were scanned with an LKB Ultrascan XL laser densitometer. Using the scanning data from the known amounts of *AQP1* insert as a standard curve, the

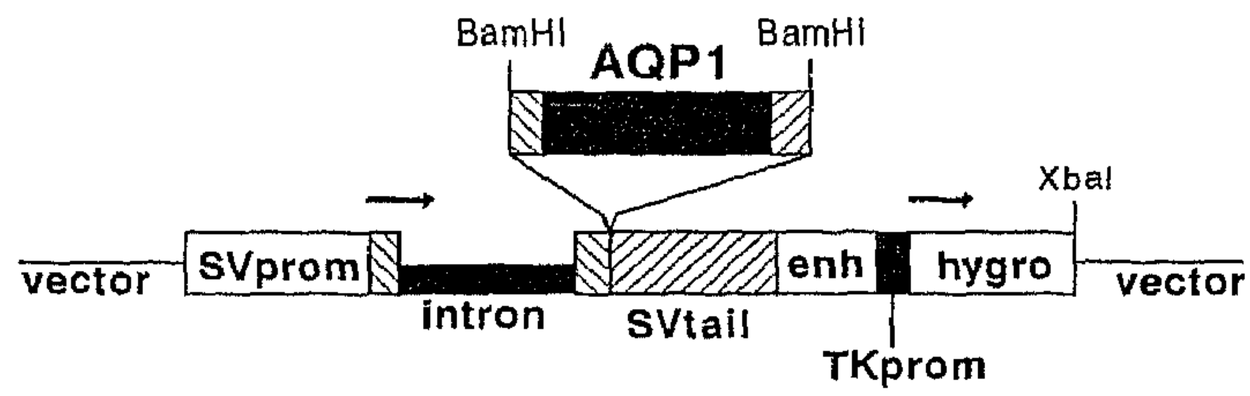

Fig. 1 Schematic drawing to scale of expression vector pSG5H*AQP1*. The SV40 early promoter (*SVprom*) and tail (*SVtail*), the rabbit β-globin intron II (*intron*), polyoma enhancer (*enh*), thymidine kinase promoter (*TKprom*), hygromycin B resistance gene (*hygro*) and *AQP1* cDNA (*AQP1*) are indicated. The 5'- and 3'-untranslated regions are *hatched*. Direction of transcription is indicated by *arrow*

amounts (in µg) of pSG5H*AQP1* integrated in genomic DNAs of the transfected cell lines were calculated. The number of copies integrated per cell was then estimated using the following formula:

$$I=(C \cdot M \cdot N \cdot G)/(F \cdot L)$$

where I is the number of copies/cell, C is the calculated amount of integrated constructs (in µg), M is the number of moles per µg DNA of 1 kbp ($1.52 \cdot 10^{-12}$) [45]. N is the number of molecules/mole (Avogadro's number: $6.0 \cdot 10^{23}$), G is the amount of genomic DNA/cell in µg ($6.6 \cdot 10^{-6}$) [27], F is the size of the hybridizing fragment (in kb) and L is the amount of genomic DNA loaded (in µg).

Northern blot analysis

Total RNA (20 µg), isolated according to Chomczynski and Sacchi [5], was resolved in a 2.2 M formaldehyde, 1% (w/v) agarose-isolated gel, transferred to a nylon membrane and UV cross-linked. Hybridization and washing conditions were as described above, except that, as a final stringency, 100 mM PO_4 buffer was used. For normalization, the blots were hybridized with a probe of a 1250-bp *Pst*I cDNA fragment coding for rat glyceraldehyde-3-phosphate dehydrogenase (GAPDH) [12]. The autoradiographic signals were scanned as described above.

Immunoblotting

Native and transfected cells were grown to confluence in 25-cm^2 dishes, scraped, washed twice with PBS and resuspended in homogenization buffer A [250 mM sucrose, 10 mM HEPES (pH=7.5), 2 mM $MgCl_2$, 1 mM EGTA, 1 mM phenyl-methyl sulphonyl fluoride, 5 µg/ml pepstatin, 80 mM sucrose] with 0.1% (w/v) SDS. Human erythrocyte ghost membranes were prepared according to Benneth [3]. After sonification, protein concentrations were determined with the BioRad protein assay. Immunoblotting of protein equivalents of 6.3 µg was done as previously described [8]. After incubation with a 1:600 dilution of monoclonal antibodies raised against dog AQP1 (kindly provided by M. L. Jennings, Texas) [21], a 1:1600 dilution of affinity-purified sheep anti-mouse immunoglobulin G (IgG) conjugated to horse radish peroxidase (Sigma Immuno Chemicals, St. Louis, Mo., USA) was used. AQP1 proteins were visualized by chemiluminescence. Scanning of the luminographic signals was done as described above.

Immuno-electronmicroscopy

Cells grown on semipermeable supports (Transwell; Costar, Badhoevedorp, The Netherlands) were fixed with 4% (w/v) paraformaldehyde in 0.1 M sodium cacodylate buffer (pH 7.2) and postfixed in 2% paraformaldehyde for 2 days. The membranes were

cut out and infiltrated for 30 min with 2.3 M sucrose containing 2% paraformaldehyde, mounted on holders and rapidly frozen in liquid nitrogen. The frozen samples were freeze-substituted [33, 36] in a Reichert AFS (Reichert, Vienna, Austria) freeze-substitution unit. Briefly, the samples were sequentially equilibrated over 3 days in 0.5% uranyl acetate in methanol at temperatures gradually decreasing from –80°C to –70°C, and then in pure methanol for 24 h at –70°C to –45°C. The samples were equilibrated at –45°C with Lowicryl HM20: methanol (1:1), at 2:1 for 2 days and finally pure HM20 (1 day) before UV-polymerization for 2 days at –40°C and 2 days at 0°C. The affinity-purified rabbit anti-human AQP1 antibodies have previously been thoroughly described for use in immunocytochemistry (kindly provided by P. Agre, Baltimore, Md., USA) [9, 34, 36]. The immunolabelling was performed using ultrathin sections (60 nm), which were pre-incubated with PBS containing 1% (w/v) bovine serum albumin (BSA) and 0.05 M glycine, and subsequently incubated with anti-AQP1 (0.1 g IgG/ml). After incubation with primary antibody overnight at 5°C, the labelling was visualized with goat anti-rabbit IgG conjugated to 10 nm colloidal gold particles (BioCell Research Laboratories, Cardiff, UK). The sections were stained with uranyl acetate for 10 min. The following controls were performed: (1) incubation with 0.1 g/ml protein-A-purified non-immune rabbit IgG; (2) pre-adsorption of antibody with excess purified AQP1 [34]; (3) incubation without use of primary antibody or without primary and secondary antibody. All controls revealed absence of labelling.

Transcellular water transport

To assay transcellular osmotic water flow, a spectroscopic method developed by Jovov et al. [22] was used. In brief, area equivalents of 1 cm^2 of cells were seeded onto transwells with a surface area of 0.33 cm^2. Then, 3 days after seeding, the apical or basolateral compartments of the transwells were washed with KHB (1.2 mM $MgSO_4$, 128 mM NaCl, 5 mM KCl, 2 mM NaH_2PO_4, 10 mM NaAc, 20 mM HEPES, 1 mM $CaCl_2$, 1 mM L-alanine, 4 mM L-lactate; pH=7.4) and filled with 150 µl of 0.5 × KHB containing 30 mg/l phenol-red or 800 µl KHB, respectively. After incubation for 2 h in a 37°C incubator, the content of the apical compartment of each well was mixed with a pipette, two aliquots of 50 µl were put into Eppendorf tubes (for duplicated measurements), diluted to 600 µl with KHB containing 2% (w/v) extran (Merck, Darmstadt, Germany) and analysed for absorbency at 479 nm (A_{479}), the isosbestic point for phenol-red [22]. A_{479} data between 0.1 and 1 correlated linearly, which is within the sample content range for the present study. Transcellular water flow (P_f in µm/s) was calculated using the following equations:

$$J_v = \left[iVol^a - \left(iVol^a \times \frac{iA^a_{479}}{eA^a_{479}} \right) \right] / t$$

$$P_f = J_v / \overline{V}_m \times A \times \Delta C$$

where J_v is the transported volume (in µl/s), Vol is volume (in µl), t is time (in s), V_m is the partial molecular volume of water (in cm^3/mol), A is area (in cm^2) and ΔC is the osmotic gradient (in mol/cm^3). Superscript a refers to "apical solution", prefix i to "initial" and prefix e to "end". Data from leaky cell layers, recognized by the presence of phenol-red in the basolateral compartment (A_{479} value ≥0.01), were omitted from water flow calculations. To investigate putative effects of PKA or PKC on transcellular osmotic water transport, both chamber compartments of *AQP1*-transfected clones contained final concentrations of 10 µM forskolin/50 µM 3-isobutyl-1-methylxanthine (IBMX) or 10 pM 12-*O*-tetradecanoyl 13-acetate (TPA), respectively, during the entire assay period. To study the effects of sulphydryl reagents on transcellular water transport, cells were fixed for 5 min in ice-cold 0.15 M cacodylate buffer (pH=7.4) containing 1% glutaraldehyde as described [11, 36], washed with KHB and assayed as described above in the presence or absence of 1 mM $HgCl_2$ in both compartments. Since fixation resulted in some leakage, data from fixed cell layers with an A_{479} value of 0.025 or less for liquid from the lower compartments were considered acceptable for water flow calculations.

Results

To generate polarized cell lines constitutively expressing AQP1, rat *AQP1* cDNA was cloned into the expression vector pSG5H, forming pSG5H*AQP1* (Fig. 1), and transfected into LLC-PK_1 and MDCK-HRS cells. Then, 10–14 days after transfection, 20 LLC-PK_1 clones and 30 MDCK-HRS clones, resistant to hygromycin B, were selected, grown to confluence in 12-well culture clusters and analysed for *AQP1* mRNA expression by Northern blotting (not shown). From the clones that gave a strong *AQP1* mRNA signal after normalization for the amount of RNA loaded, LLC-PK_1 clone 7 and MDCK-HRS clone K were selected for further analyses.

To estimate the number of pSG5H*AQP1* constructs integrated into the genomes of clones 7 and K, genomic DNAs of non-transfected LLC-PK_1 and MDCK-HRS cells and clones 7 and K were isolated, digested with *Bam*HI and analysed by Southern blot analysis together with known amounts of *AQP1* cDNA inserts (Fig. 2). Hybridization with a 1044-bp *AQP1* cDNA probe demonstrated a single band of approximately 1 kb in the lanes containing genomic DNAs of the transfected clones, which corresponds to the size of the *AQP1* insert. No *AQP1*-specific signal was detected in lanes loaded with genomic DNAs from non-transfected cells. Densitometric scanning of the *AQP1* hybridization signals and subsequent calculations revealed that in clone 7 about two copies, and in clone K about one copy, per cell were integrated.

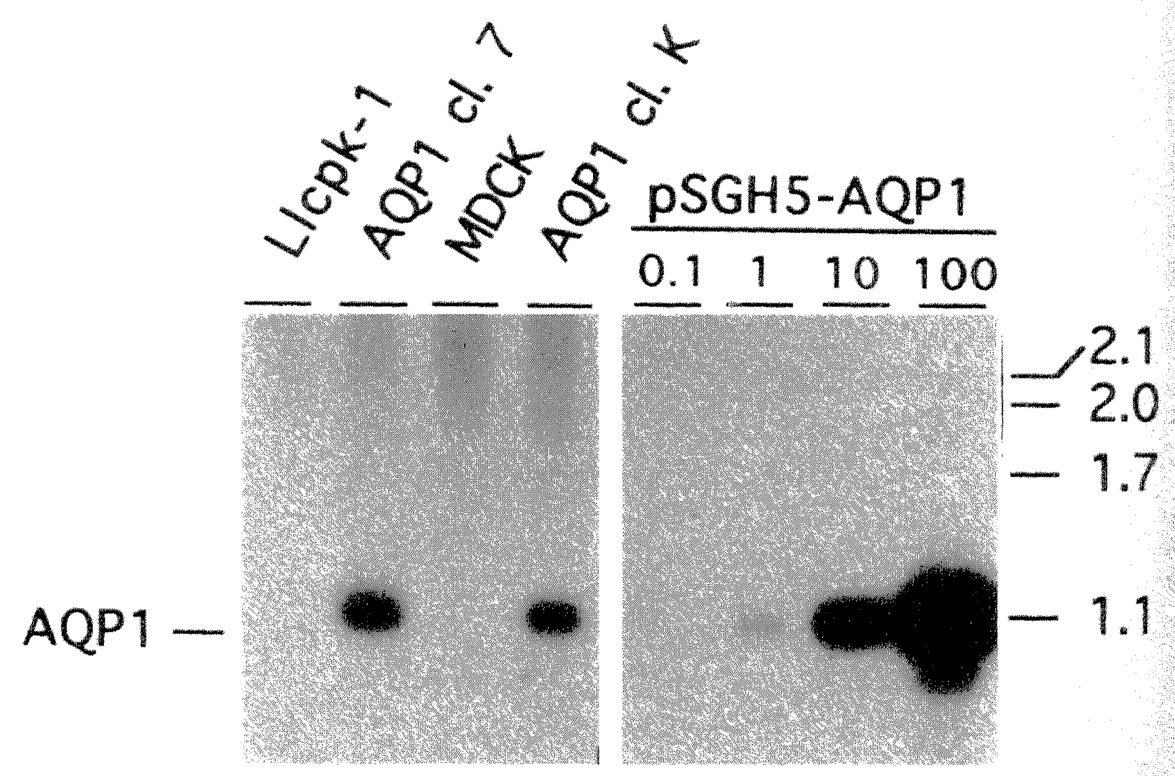

Fig. 2 Southern blot analysis of genomic DNAs isolated from LLC-PK_1, MDCK-HRS, or *AQP1*-transfected clones 7 or K. Genomic DNA (10 µg) was digested with *Bam*HI, separated on a gel, blotted and hybridized with an [α-^{32}P]-labelled *AQP1* probe. To determine the copy number of pSG5H*AQP1* integrated, 0.1, 1, 10 or 100 pg *AQP1* insert was also loaded on the gel. Sizes of fragments of *Pst*I-digested lambda DNA are indicated to the right (in Kb)

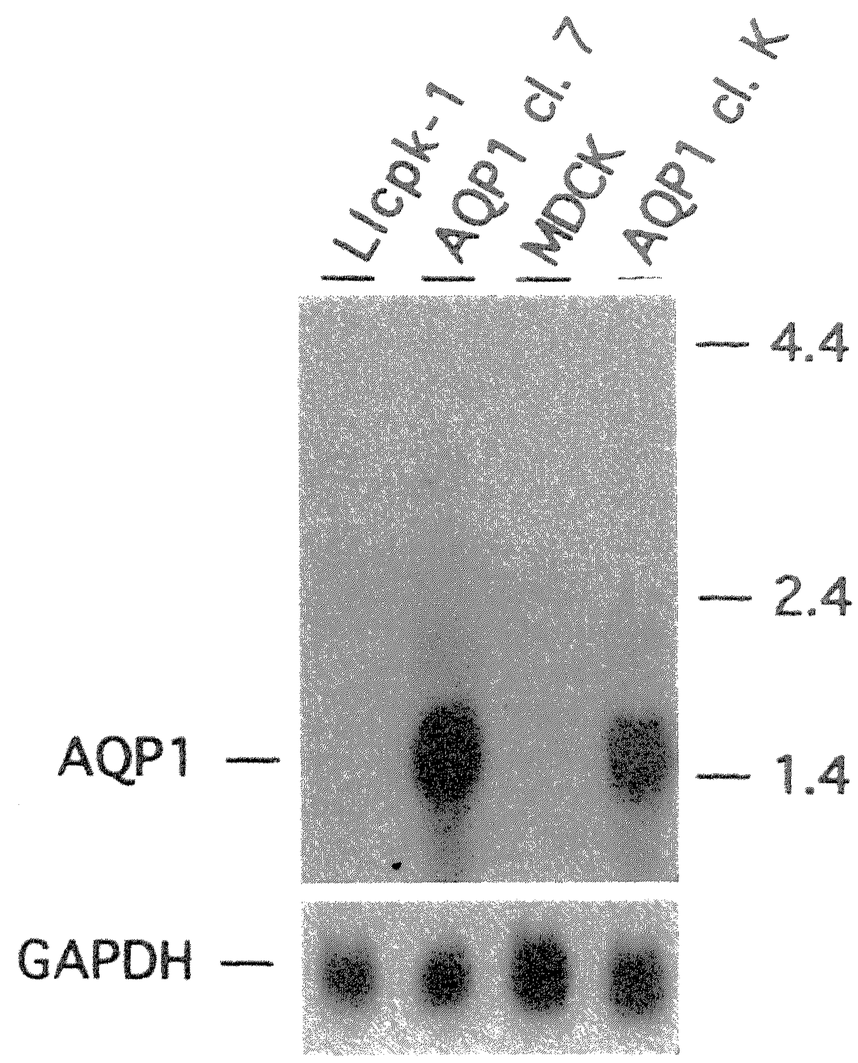

Fig. 3 Northern blot analysis of RNA isolated from LLC-PK_1, MDCK-HRS, or *AQP1*-transfected clones 7 or K. RNA (20 μg) was separated on a 2.2 M formaldehyde, 1% (w/v) agarose gel and transferred to a nylon membrane. After UV cross-linking the blot was hybridized as described in Fig. 2. For normalization the blot was also hybridized with a rat glyceraldehyde-3-phosphate dehydrogenase (*GAPDH*) probe. Sizes of RNA marker (GIBCO-BRL) are indicated to the right (in Kb)

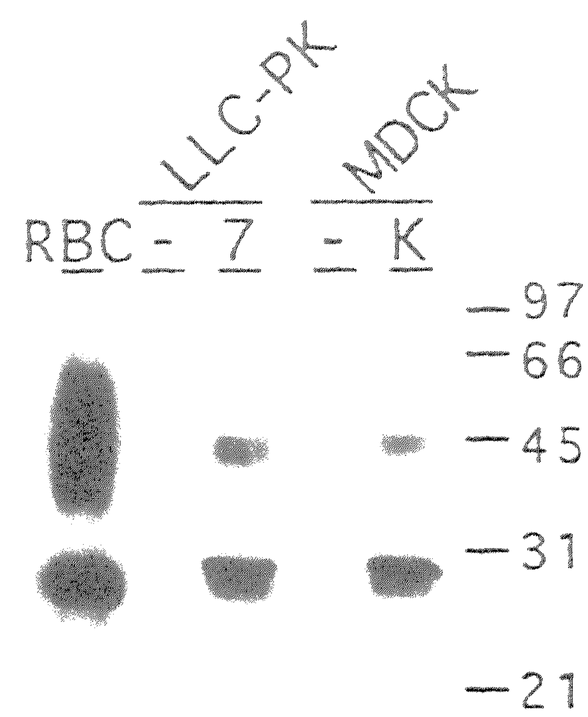

Fig. 4 Immunoblot analysis of the AQP1 expression in LLC-PK_1, MDCK-HRS, or *AQP1*-transfected clones 7 or K. Protein equivalents (6.3 μg) were separated by SDS-PAGE and blotted onto a nitrocellulose membrane. AQP1 proteins were visualized by chemiluminescence detection using mouse monoclonal antibodies raised against dog AQP1 as a first antibody and sheep anti-mouse-IgG conjugated to horse radish peroxidase, as a second antibody. As a positive control, 6.3 μg of human erythrocyte ghost membranes was loaded. The molecular mass (in kDa) of low-molecular-weight marker proteins (GIBCO-BRL) is indicated

Northern blot analysis of RNA isolated from native cells and clones 7 and K revealed a single mRNA species of approximately 1.5 kb, which was recognized by the *AQP1* probe (Fig. 3). No *AQP1*-specific signal could be detected in the lanes containing RNA from the native cell lines. After normalization for the loaded amount of mRNA, *AQP1* mRNA expression in clone 7 was approximately two times higher than in clone K.

To determine the expression levels of AQP1 in clones 7 and K, homogenates of native and clonal cells were subjected to immunoblot analysis (Fig. 4). Staining with Ponceau Red showed that equal amounts of protein were loaded (not shown). Chemiluminescence detection with a monoclonal antibody directed against dog AQP1 demonstrated proteins of about 28 kDa and 40–45 kDa in both lanes of the *AQP1*-transfected clones and that of red blood cell membranes, while no protein was detected in the lanes of the native cells. Densitometric scanning revealed that the amounts of AQP1 were similar in both clonal cell lines. Similar results were obtained when affinity-purified rabbit anti-AQP1 antibodies were used (not shown).

To analyse the subcellular localization of AQP1 within the clonal cells, immunocytochemistry was performed with affinity-purified rabbit AQP1 antibodies. Specific and extensive immunogold labelling in apical and basolateral membranes and vesicular structures of clone K was demonstrated (Fig. 5A). Staining was absent in negative controls in which non-immune IgG was used instead of anti-AQP1 (Fig. 5B) or in sections of the native cell lines (Fig. 5C). Identical data were obtained for clone 7 (not shown).

Since AQP1 appeared to be distributed to the apical and basolateral membranes in the *AQP1*-transfected clones, clonal and native cell lines were seeded on permeable inserts and analysed for transcellular osmotic water permeability, P_f (in μm/s ± SEM), using phenol-red as a concentration marker (Fig. 6; shows only clone K). After an incubation period of 2 h, the P_f values were 58 ± 1 and 57 ± 1 μm/s for clone K and 7, respectively. In contrast, P_f values for cell layers of non-transfected MDCK and LLC-PK_1 cells were only 4 ± 2 μm/s for both types. Since osmotic water permeability through AQP1, but not diffusion through lipid bilayers, is inhibited by mercurial sulphydryl reagents [32, 41, 46], the effect of these compounds on transcellular water transport was studied (Fig. 6). Incubation of clone K cells with 1 mM $HgCl_2$ during the 2-h assay period resulted in cell death, as concluded from the complete equilibration of phenol-red across the cell layer (not shown). To avoid toxic effects on living cells, the cells were pre-treated with glutaraldehyde, a treatment which has been shown to preserve water permeability characteristics of urinary bladders and renal descending vasa recta [11, 36, 47]. This fixation led to a somewhat reduced, but consistently high, P_f, which could be totally blocked by mercurial compounds without a further leakage of phenol-red (Fig. 6). With control MDCK cells, $HgCl_2$ did not alter its P_f (Fig. 6). Identical results were obtained with 3 mM $HgCl_2$ and with 1 or 3 mM *p*-chloromercuribenzene sulphonate (pCMBS; not shown). Data for clone 7 cells were the same (not shown).

In the primary structure of AQP1, two putative PKC phosphorylation sites have been recognized. To test whether PKC or PKA influences water permeation

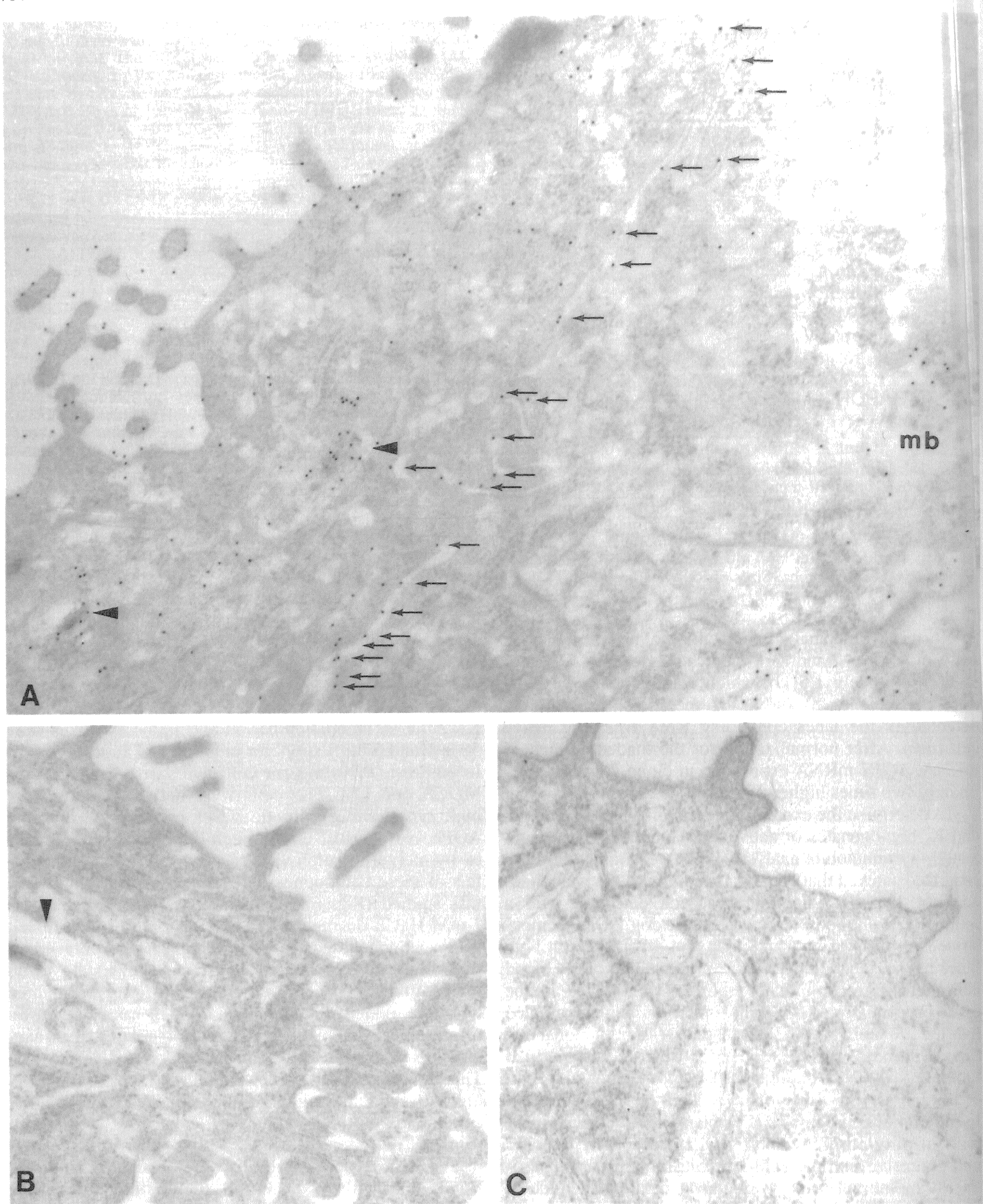

Fig. 5A–C Immuno-electronmicrographs of *AQP1*-transfected clone K and non-transfected MDCK cells. **A** In clone K cells, extensive labelling of AQP1 is seen on the entire apical plasma membrane, including microvilli projections, and on the basolateral plasma membrane (*arrows*). In addition, numerous small vesicular structures and larger multivesicular bodies (*mb*, *arrowheads*) are also extensively labelled, ×40,000. **B** No labelling is seen in immunolabelling control incubated with non-immune immunoglobulin G (IgG), ×40,000. **C** Non-transfected MDCK cells reveal only very sparse or no labelling, ×50,000

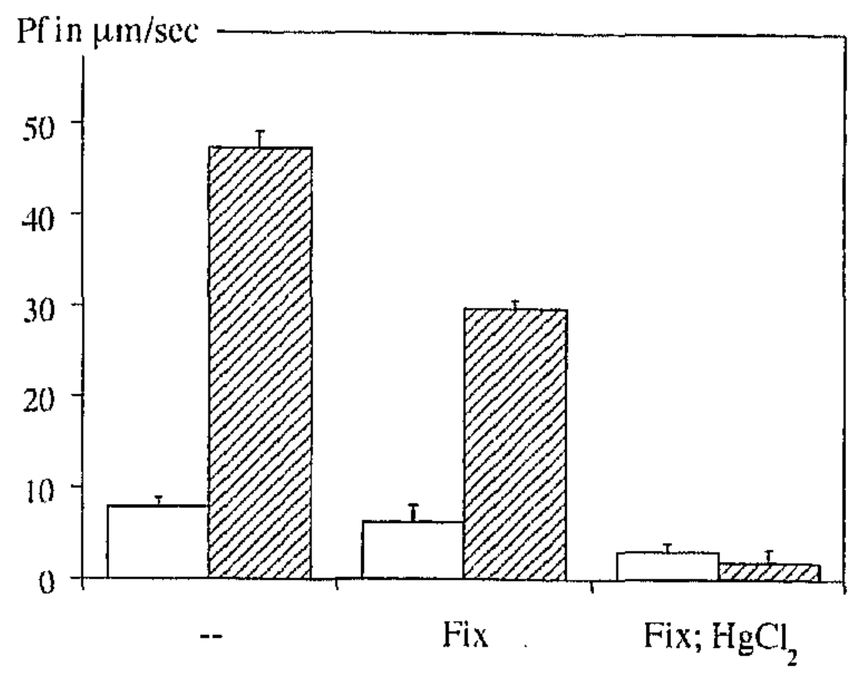

Fig. 6 Inhibition of transcellular osmotic water permeability (P_f) of native MDCK or *AQP1*-transfected clone K cells with $HgCl_2$. MDCK cells (*open bars*) or clone K cells (*hatched bars*) were not pre-treated and assayed (–) or were fixed with 1% glutaraldehyde for 5 min (*Fix*) and assayed in the presence (*$HgCl_2$*) or absence (not indicated) of 1 mM $HgCl_2$. The P_f is expressed in µm/s ± SEM; n=3

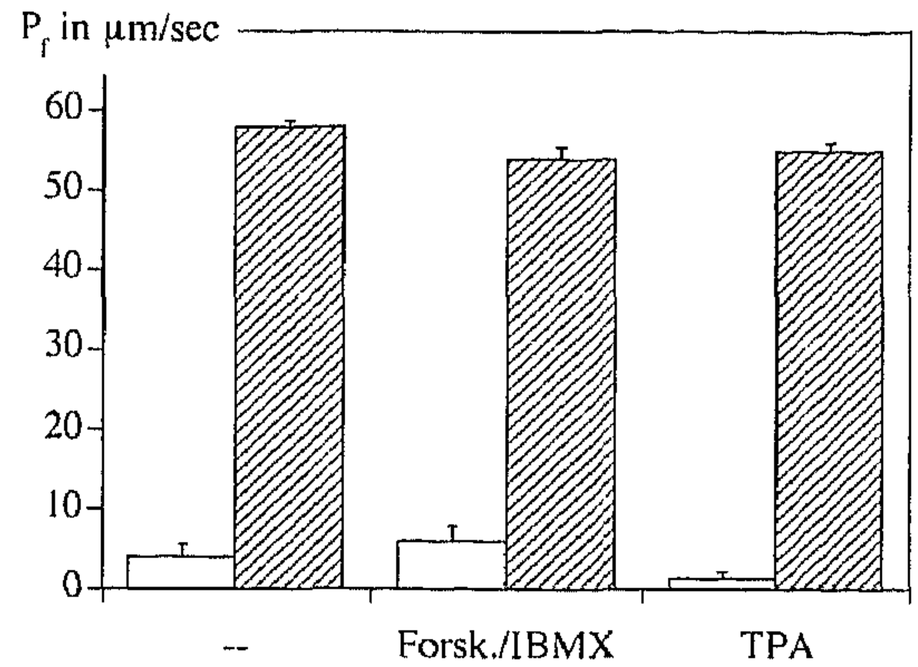

Fig. 7 Transcellular osmotic water permeabilities (P_f) of native MDCK or *AQP1*-tranfected clone K cells. MDCK cells (*open bars*) or clone K cells (*hatched bars*) were incubated without additives (–), with 10 µM forskolin/50 µM IBMX (*Forsk./IBMX*) or with 10 pM TPA (*TPA*). The P_f is expressed in µm/s ± SEM; n=3

through AQP1, clonal cells were incubated with either 10 pM TPA or 10 µM forskolin/50 µM IBMX, respectively. This treatment, however, had no effect on transcellular P_f values of clone K (Fig. 7) or clone 7 cells (not shown). Higher concentrations of TPA or forskolin resulted in phenol-red leakage (not shown), which might be due to a changed cytoskeleton structure [13, 26].

Discussion

The development and maintenance of epithelial polarity requires the continuous sorting of newly synthesized and internalized plasma membrane components. The polarized MDCK cell line, and to a lesser extent the LLC-PK_1 cell line, has been used extensively as a model to study biogenesis of membrane polarity and for targeting of endogenous and exogenous proteins in epithelial cells [19, 29, 30, 42]. In the present study, we generated and analysed MDCK and LLC-PK_1 clones, which were stably transfected with an AQP1 expression construct. The number of expression constructs integrated per cell, which was one for MDCK clone K and two for LLC-PK_1 clone 7 (Fig. 2), was reflected in the relative amount of *AQP1* mRNA expressed in these clones (Fig. 3), but not in the relative amounts of AQP1 protein synthesized. In both clones AQP1 was expressed at comparable levels (Fig. 4). The discrepancy between the relative *AQP1* mRNA and protein levels in both clones might be due to a difference in translational efficiency and/or stability of AQP1 in these two cell types.

Although MDCK and LLC-PK_1 cells secrete endogenous plasminogen activators from opposite cell surfaces [39], many specific recombinant proteins are targeted to the same surface in these cell lines [19, 30, 42]. Furthermore, targeting of a recombinant protein in these polarized cell lines is very similar to that found in the native tissue of expression [19, 29, 30]. In the present study we showed that this also holds for AQP1. As in proximal tubules [34, 40], AQP1 labelling was found in the apical and basolateral membranes and in endocytic vesicles of cells from LLC-PK_1 clone 7 as well as MDCK clone K (Fig. 5). This similar localization suggests that, when a targeting signal is essential for routing to both surfaces of the cell, this signal is contained within the primary structure of AQP1 and correct targeting of AQP1 seems, therefore, to be cell-type independent.

To study transcellular water permeability, we adapted a spectroscopic method utilizing cell-impermeant phenol-red as a concentration marker. Application of this method revealed similar transcellular osmotic water permeabilities for both clones, which were more than 12 times higher than those of the corresponding non-transfected cell lines. Considering the unstirred layers present in our system, the measured P_f values must be underestimated [4]. The relatively low P_f of our transfected cells compared to those of isolated renal proximal tubules [38] might be explained by effects of these unstirred layers and/or differences in AQP1 expression levels.

A characteristic of AQP1-mediated water flow is its inhibition by mercurial compounds. In vivo, measurements of transcellular P_f are difficult to pursue, because mercurial compounds are toxic to cells. Also in our system, addition of $HgCl_2$ was deleterious for the cells, but this effect could be prevented by pre-fixation with glutaraldehyde. This treatment resulted in some leakage of phenol-red to the basolateral compartment, presumably caused by loss of contact between the cells and the plastic support surrounding them and which might explain the reduction in P_f. However, the inhibition by mercurial compounds of P_f of both clonal cells and the low basal P_f of the non-transfected cells are proof that the observed high water permeabilities must be conferred by AQP1. This demonstrates for the first time that transepithelial water transport in cultured cells can be blocked by mercurial compounds.

Electron microscopy of clone K and clone 7 cells localized AQP1, to intracellular vesicles, as well as to plasma membranes. In renal collecting duct cells it is well established that PKA triggers the fusion of intracellular vesicles containing AQP2 water channels with the apical membrane, resulting in an increased transcellular water flow. In proximal tubules it has been shown that endocytosis can be modulated by PKC [37]. AQP1 contains two PKC consensus sequences [6]. Analysis of clone K and clone 7 cells revealed, however, that activation of phosphorylation by PKA or PKC did not influence AQP1-mediated transcellular osmotic water permeability (Fig. 7). This is in line with the constitutive nature of AQP1 expression in proximal tubules. Similar results with PKA were noted for AQP1 expressed in CHO cells [31] and LLC-PK_1 cells [24].

In conclusion, we have shown that in transfected MDCK and LLC-PK_1 cells AQP1 is distributed as described for proximal tubule cells. In addition, a simple spectroscopic assay [22] was applied, with which AQP1-mediated transcellular water permeability in these clones and the effects of mercurial compounds on it were examined. In vivo, AQP1–4 are targeted to different compartments of the cell and they are regulated differently. This might also be mimicked in transfected epithelial cells. In fact, vasopressin-regulated shuttling of AQP2 to the plasma membrane in transfected LLC-PK_1 cells has already been shown [24, 25]. The described spectroscopic assay will be a valuable tool to study (the regulation of) transcellular water flow mediated by these AQPs in the transfected cells. Furthermore, these transfected cells will provide useful models with which to unravel the mechanisms involved in intracellular routing in general and of water channels in particular.

Acknowledgements This study was supported by the Dutch Kidney Foundation (C93.1299) and the Novo Nordisk Foundation. We thank H. van Boxtel and I. Kristoffersen for technical assistance, Dr E. Sistermans (Department of Cell Biology, University of Nijmegen) for construction of pSG5H. Dr M.L. Jennings (Dept. of Physiology and Biophysics, University of Texas, Galveston) and Dr. P. Agre (Dept. of Medicine and Cell Biology, Johns Hopkins University, Baltimore) are acknowledged for their generous gifts of monoclonal AQP1 antibodies and rabbit AQP1 antibodies, respectively.

References

1. Agre P, Preston GM, Smith BL, Jung JS, Raina S, Moon C, Guggino WB, Nielsen S (1993) Aquaporin CHIP: the archetypal molecular water channel. Am J Physiol 265:F463–F476
2. Belt PB, Groeneveld H, Teubel WJ, van de Putte P, Backendorf C (1989) Construction and properties of an Epstein-Barr-virus-derived cDNA expression vector for human cells. Gene 84:407–417
3. Benneth V (1983) Proteins involved in membrane-cytoskeleton association in human erythrocyte: spectrin, ankyrin, and band 3. Methods Enzymol 96:313–324
4. Berry CA (1983) Water permeability and pathways in the proximal tubule. Am J Physiol 245:F279–F294
5. Chomczynski P, Sacchi N (1987) Single-step method of RNA isolation by acid guanidinium thiocyanate-phenol-chloroform extraction. Anal Biochem 162:156–159
6. Deen PM, Dempster JA, Wieringa B, van Os CH (1992) Isolation of a cDNA for rat CHIP28 water channel: high mRNA expression in kidney cortex and inner medulla. Biochem Biophys Res Commun 188:1267–1273
7. Deen PM, Verdijk MA, Knoers NV, Wieringa B, Monnens LA, van Os CH, van Oost BA (1994) Requirement of human renal water channel aquaporin-2 for vasopressin-dependent concentration of urine. Science 264:92–95
8. Deen PM, Croes H, van Aubel RA, Ginsel LA, van Os CH (1995) Water channels encoded by mutant aquaporin-2 genes in nephrogenic diabetes insipidus are impaired in their cellular routing. J Clin Invest 95:2291–2296
9. Denker BM, Smith BL, Kuhajda FP, Agre P (1988) Identification, purification, and partial characterization of a novel Mr 28,000 integral membrane protein from erythrocytes and renal tubules. J Biol Chem 263:15634–15642
10. Echevarria M, Windhager EE, Tate SS, Frindt G (1994) Cloning and expression of AQP3, a water channel from the medullary collecting duct of rat kidney. Proc Natl Acad Sci USA 91:10997–11001
11. Eggena P (1972) Glutaraldehyde-fixation method for determining the permeability to water of the toad urinary bladder. Endocrinology 91:240–246
12. Fort P, Marty L, Piechaczyk M, el Sabrouty S, Dani C, Jeanteur P, Blanchard JM (1985) Various rat adult tissues express only one major mRNA species from the glyceraldehyde-3-phosphate-dehydrogenase multigenic family. Nucleic Acids Res 13:1431–1442
13. Fritz BA, Lowe AW (1996) Polarized GP2 secretion in MDCK cells via GPI targeting and apical membrane-restricted proteolysis. Am J Physiol 33:G176–G183
14. Fujimura FK, Deininger PL, Friedmann T, Linney E (1981) Mutation near the polyoma DNA replication origin permits productive infection of F9 embryonal carcinoma cells. Cell 23:809–814
15. Fushimi K, Uchida S, Hara Y, Hirata Y, Marumo F, Sasaki S (1993) Cloning and expression of apical membrane water channel of rat kidney collecting tubule. Nature 361:549–552
16. Graham FL, Eb AJ (1973) A new technique for the assay of infectivity of human adenovirus 5 DNA. Virology 52:456–467
17. Green S, Issemann I, Sheer E (1988) A versatile in vivo and in vitro eukaryotic expression vector for protein engineering. Nucleic Acids Res 16:369
18. Hasegawa H, Ma T, Skach W, Matthay MA, Verkman AS (1994) Molecular cloning of a mercurial-insensitive water channel expressed in selected water-transporting tissues. J Biol Chem 269:5497–5500
19. Horio M, Chin KV, Currier SJ, Goldenberg S, Williams C, Pastan I, Gottesman MM, Handler J (1989) Transepithelial transport of drugs by the multidrug transporter in cultured Madin-Darby canine kidney cell epithelia. J Biol Chem 264: 14880–14884
20. Ishibashi K, Sasaki S, Fushimi K, Uchida S, Kuwahara M, Saito H, Furukawa T, Nakajima K, Yamaguchi Y, Gojobori T et al. (1994) Molecular cloning and expression of a member of the aquaporin family with permeability to glycerol and urea in addition to water expressed at the basolateral membrane of kidney collecting duct cells. Proc Natl Acad Sci USA 91: 6269–6273
21. Jennings ML (1992) Monoclonal antibody against red blood cell CHIP28 protein (abstract). J Gen Physiol 100:21A
22. Jovov B, Wills NK, Lewis SA (1991) A spectroscopic method for assessing confluence of epithelial cells. Am J Physiol 261:C1196–C1203
23. Jung JS, Bhat RV, Preston GM, Guggino WB, Baraban JM, Agre P (1994) Molecular characterization of an aquaporin cDNA from brain: candidate osmoreceptor and regulator of water balance. Proc Natl Acad Sci USA 91:13052–13056
24. Katsura T, Verbavatz JM, Farinas J, Ma T, Ausiello DA, Verkman AS, Brown D (1995) Constitutive and regulated membrane expression of aquaporin 1 and aquaporin 2 water channels in stably transfected LLC–K1 epithelial cells. Proc Natl Acad Sci USA 92:7212–7216

25. Katsura T, Ausiello DA, Brown D (1996) Direct demonstration of aquaporin-2 water channel recycling in stably transfected LLC-PK1 epithelial cells. Am J Physiol 39:F548–F553
26. Kelly S, Holme TC, Bissell MJ (1985) Interaction of tumour promoters with epithelial cells in culture. An immunofluorescence study. Exp Cell Res 160:159–174
27. Lewin B (1990) About genomes and chromosomes. In: Genes IV. Oxford University Press and Cell Press, New York, pp 390
28. van Lieburg AF, Verdijk MA, Knoers VV, van Essen AJ, Proesmans W, Mallmann R, Monnens LA, van Oost BA, van Os CH, Deen PM (1994) Patients with autosomal nephrogenic diabetes insipidus homozygous for mutations in the aquaporin 2 water-channel gene. Am J Hum Genet 55:648–652
29. Lisanti MP, Sargiacomo M, Graeve L, Saltiel AR, Rodriguez Boulan E (1988) Polarized apical distribution of glycosyl-phosphatidylinositol-anchored proteins in a renal epithelial cell line. Proc Natl Acad Sci USA 85:9557–9561
30. Low SH, Wong SH, Tang BL, Hong WJ (1991) Involvement of both vectorial and transcytotic pathways in the preferential apical cell surface localization of rat dipeptidyl peptidase IV in transfected LLC-PK1 cells. J Biol Chem 266:19710–19716
31. Ma T, Frigeri A, Tsai ST, Verbavatz JM, Verkman AS (1993) Localization and functional analysis of CHIP28k water channels in stably transfected Chinese hamster ovary cells. J Biol Chem 268:22756–22764
32. Macey RI (1984) Transport of water and urea in red blood cells. Am J Physiol 246:C195–C203
33. Maunsbach AB (1994) Embedding of cells and tissues for ultrastructural and immunocytochemical analysis. In: Celis JE (ed) Cell biology: a laboratory handbook. Academic, Orlando, Fla., pp 117–125
34. Nielsen S, Smith BL, Christensen EI, Knepper MA, Agre P (1993) CHIP28 water channels are localized in constitutively water-permeable segments of the nephron. J Cell Biol 120: 371–383
35. Nielsen S, Chou CL, Marples D, Christensen EI, Kishore BK, Knepper MA (1995) Vasopressin increases water permeability of kidney collecting duct by inducing translocation of aquaporin-CD water channels to plasma membrane. Proc Natl Acad Sci USA 92:1013–1017
36. Nielsen S, Pallone T, Smith BL, Christensen EI, Agre P, Maunsbach AB (1995) Aquaporin-1 water channels in short and long loop descending thin limbs and in descending vasa recta in rat kidney. Am J Physiol 268:F1023–F1037
37. O'Neil RG, Reid JM (1988) Cell swelling and a diacylglycerol analogue activate endocytosis in renal proximal straight tubule (abstract). FASEB J 2:A1284
38. van Os CH, Deen PM, Dempster JA (1994) Aquaporins: water selective channels in biological membranes. Molecular structure and tissue distribution. Biochim Biophys Acta 1197: 291–309
39. Ragno P, Estreicher A, Gos A, Wohlwend A, Belin D, Vassalli JD (1992) Polarized secretion of urokinase-type plasminogen activator by epithelial cells. Exp Cell Res 203:236–243
40. Sabolic I, Valenti G, Verbavatz JM, Van Hoek AN, Verkman AS, Ausiello DA, Brown D (1992) Localization of the CHIP28 water channel in rat kidney. Am J Physiol 263: C1225–C1233
41. Solomon AK, Chasan B, Dix JA, Lukacovic MF, Toon MR, Verkman AS (1983) The aqueous pore in the red cell membrane: band 3 as a channel for anions, cations, nonelectrolytes, and water. Ann NY Acad Sci 414:97–124
42. Tanigawara Y, Okamura N, Hirai M, Yasuhara M, Ueda K, Kioka N, Komano T, Hori R (1992) Transport of digoxin by human P-glycoprotein expressed in a porcine kidney epithelial cell line (LLC-PK1). J Pharmacol Exp Ther 263:840–845
43. Terris J, Ecelbarger CA, Marples D, Knepper MA, Nielsen S (1995) Distribution of aquaporin-4 water channel expression within rat kidney. Am J Physiol 38:F775–F785
44. Thomas KR, Capecchi MR (1987) Site-directed mutagenesis by gene targeting in mouse embryo-derived stem cells. Cell 51:503–512
45. Titus DE (1991) In: Promega protocols and applications guide. Promega, Madison, Wis.
46. Verkman AS (1989) Mechanisms and regulation of water permeability in renal epithelia. Am J Physiol 257:C837–C850
47. Wade JB, Kachadorian WA (1988) Cytochalasin B inhibition of toad bladder apical membrane responses to ADH. Am J Physiol 255:C526–C530